NANO LETTERS

Letter

pubs.acs.org/NanoLett

Two-Color Antibunching from Band-Gap Engineered Colloidal Semiconductor Nanocrystals

Zvicka Deutsch,*[,1] Osip Schwartz,[1] Ron Tenne,[1] Ronit Popovitz-Biro,[2] and Dan Oron[1]

[1]Department of Physics of Complex Systems and [2]Electron Microscopy Unit, Weizmann Institute of Science, Rehovot 76100, Israel

Supporting Information

ABSTRACT: Photon antibunching is ubiquitously observed in light emitted from quantum systems but is usually associated only with the lowest excited state of the emitter. Here, we devise a fluorophore that upon photoexcitation emits in either one of two distinct colors but exhibits strong antibunching between the two. This work demonstrates the possibility of creating room-temperature quantum emitters with higher complexity than effective two level systems via colloidal synthesis.

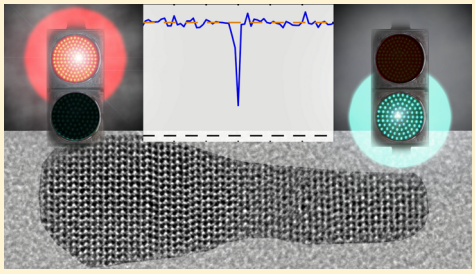

KEYWORDS: *Quantum dots, antibunching, dual-emission, colloidal synthesis, Auger recombination, multiexcitons*

One of the defining features of a light source is the statistics of its photon emission. Thermal or pseudothermal light sources exhibit positive correlation between photon detection events in the time scale reciprocal to the bandwidth of light, a phenomenon known as "photon bunching".[1−3] Coherent light sources, such as lasers, demonstrate no such correlations.[2] In contrast with both, which can be described within a classical framework, light from individual fluorescent emitters typically exhibits negative correlations known as antibunching,[4] associated with sub-Poissonian statistics.[5] This inherently quantum phenomenon stems from the distinctive property of quantum emitters to emit photons one at a time.

Since its first observation over 30 years ago from atomic systems,[4] photon antibunching has been observed from a variety of quantum emitters. Observation of photon antibunching from single organic dye molecules[6] marked the dawn of the age of single molecule spectroscopy, since it is the definitive method for confirming the detection of a single emitter. Later, solid-state sources such as color centers[7] and semiconductor quantum dots[8,9] were also shown to exhibit antibunching. Solid-state quantum emitters have been extensively studied over the past decade in the broader context of constructing new types of nonclassical light sources, which are of utmost importance to applications in quantum cryptography and quantum communication.[2] These include solid-state devices able to emit single photons[10] and entangled photon pairs[11,12] "on demand".

In most antibunching experiments, light emission is observed only from the lowest excited state ("Kasha's rule"). This is true even for systems in which two emitters (emitting individually at a different color) are combined and coupled with one another as has been demonstrated, for example, in multichromophoric coupled organic dye systems.[13−16]

Here we employ advanced colloidal synthesis methods in conjunction with band gap engineering to produce a solid-state fluorophore emitting in two distinct spectral bands and exhibiting antibunching between them. Such behavior is referred to throughout this paper as two-color antibunching. The fluorophore is based on a composite semiconductor nanocrystal incorporating two separately emitting components that are coupled via Coulomb-mediated exciton−exciton interactions.

A two-color emitting fluorophore requires, essentially, the combination of two subsystems emitting at different colors. A variant of such systems was recently realized with colloidal quantum dots by first depositing a thick shell of a wide band gap material on a spherical quantum dot to form a typical core−shell structure, and then growing an outer layer of a lower band gap material to form an independently emitting quantum well, resulting in the structure depicted in Figure 1a.[17,18]

However, to achieve photon correlations between the two emitters a coupling mechanism is required.[16] It must strongly affect the emission properties (e.g., emission color, lifetime, or quantum yield) of at least one of the two emitters upon photoexcitation of both. A potential candidate for such coupling, which is unique to colloidal QDs, is Auger recombination.[19] As depicted in Figure 1b, when more than two charge carriers are present in a strongly confined QD, carrier relaxation is dominated by a nonradiative decay channel. Energy from recombination of an exciton is transferred to a spectator charge rather than being released as a photon. Auger recombination is responsible for the extremely reduced emission quantum yields observed from multiply excited states of colloidal QDs.

In this context, we envisaged an alternative design for a two-color emitting system, introduced schematically in Figure 1c,

Received: February 15, 2012
Revised: April 22, 2012
Published: April 25, 2012

   dx.doi.org/10.1021/nl300638t | *Nano Lett.* 2012, 12, 2948−2952

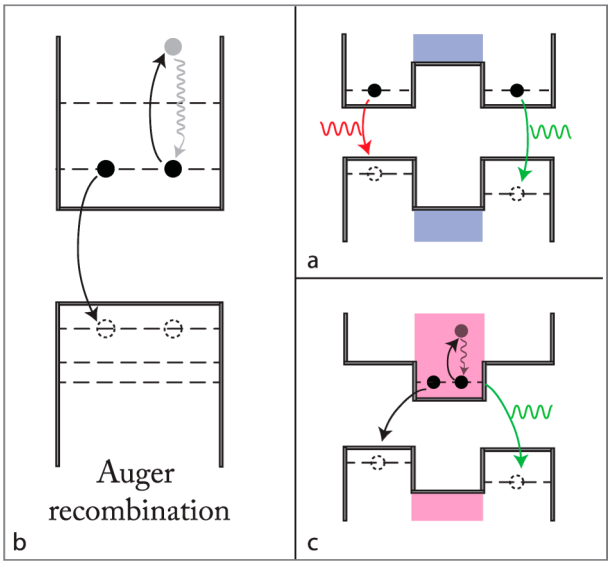

Figure 1. Schematic band diagrams of dual emitting systems. (a) Band diagram for a dual-color emitting fluorophore in which two excitons are spatially well separated by a thick tunneling barrier in both the valence and the conduction band. (b) Energy level diagram depicting Auger recombination. Upon recombination of an exciton the released energy leads to further excitation of a spectator charge carrier, which then rapidly cools to the band edge via phonons. (c) Band diagram for a dual-color emitting fluorophore in which the electrons are spatially localized in a single region whereas holes are separated by a thick tunneling barrier. In this system, trion Auger recombination can efficiently occur between two electrons and one of the holes, strongly suppressing simultaneous dual-color emission. This is schematically shown for the case in which the hole on the left recombines nonradiatively leaving an electron and the hole on the right free to recombine radiatively.

which exploits Auger recombination as the coupling mechanism. Here, one type of charge carriers (e.g., holes) is confined by a double-well potential, essentially splitting carriers into two spatially distinct regions, while the oppositely charged carrier is localized in a single region. While this system is capable of emitting in two colors, due to the nondegenerate valence band positions of the two regions, simultaneous two-color emission is expected to be significantly inhibited. When both emitters are simultaneously excited, each of them is essentially occupied by a trion, which undergoes rapid Auger decay, as depicted in Figure 1c. Thus, no more than a single photon is emitted despite the double excitation of the QD. The probability to emit either a "green" or a "red" photon is determined in this case by the ratio of nonradiative recombination rates of the two trion systems and by the rate of FRET from the higher energy well to the lower energy one.

We have experimentally realized the system schematically depicted in Figure 1c using exclusively II–VI semiconductors for which synthetic protocols are highly evolved. As shown in Figure 2a, we chose to work with CdS (predominantly) as the barrier layer and both CdSe and CdZnSe as the hole localizing regions. To generate a significant spectral shift between the two emission bands, the CdSe core is isovalently doped by tellurium, leading to substantially red-shifted emission.[20] This choice also significantly mitigates FRET between the two emission centers, as the absorption edge is hardly affected by doping.

The theoretical system presented schematically in Figure 1c differs slightly from our actualized system in that in the former the electrons are localized exclusively within the barrier shell, whereas in the latter the electrons inhabit both the core and the barrier. This, however, is inconsequential for the trion-based coupling mechanism described above.

A brief summary of the synthetic procedure is provided below, while a detailed account is given in the Supporting Information. Spherical Te-doped CdSe QDs,[20] having a 3 nm diameter and emitting at 620 nm (see TEM image in Figure 2(c1)), are used as seeds for overgrowth of a thick CdS layer, which transforms them into ellipsoidal particles with axes of 7.5 and 3.5 nm (not shown). As has been recently shown, this choice of core size in a CdSe/CdS seeded rod leads to significant delocalization of the electron into CdS,[21] an imperative prerequisite for producing overlap between electrons in the core and holes in an external shell beyond the barrier (as portrayed schematically in Figure 1c). Electron delocalization is indeed confirmed by observation of a 60 nm redshift in the emission throughout the course of the CdS growth stage. These NCs were grown further by deposition of additional CdS on top of the existing seeded-grown CdS layer, resulting in chunky rod-shaped particles (Figure 2c2). Upon growth of CdZnSe alloy as an external layer, significant emission is expected to emanate from the CdS/CdZnSe interface. Indeed, a second emission peak appears at 580 nm as seen in the emission spectrum depicted in Figure 2b. CdZnSe growth is initially seen as a thin extension protruding from the seeded rods (Figure 2c3). Further growth leads mostly to the lengthening and thickening of this protrusion (Figure 2c4) and at later stages to formation of additional lobes on the opposite end of the rods (Figure 2c5). Throughout CdZnSe growth, the two emission colors remain completely distinguishable, providing easy access to optical studies on two color emission. The higher energy emission peak becomes more dominant as growth progresses due to the increased probability of absorption in the CdZnSe layer. The overall quantum yield (QY) of the QDs was estimated to be about 5% by comparing to fluorescence of a dye standard. Measurements were performed using 532 nm excitation and the branching ratio between NIR and Vis emissions was found to be 4:1 (see further details in the Supporting Information).

For optical studies of single QD emission, we chose to work with the particles depicted in Figure 2c4, where CdZnSe growth is significant but multiple CdZnSe arms are mostly not present. Briefly, samples were prepared for optical measurements by spin coating a dilute solution of QDs in PMMA on precleaned glass slides. Luminescence was excited by a pulsed diode laser operated at 5 MHz. Luminescence was epi-detected through an oil immersion objective. Wide-field excitation was used to locate individual QDs. A fiber-coupled spectrometer was used to measure single QD spectra, whereas a modified Hanbury-Brown Twiss detection scheme was used to characterize emission statistics. Emitted light was first split by a 650 nm long-pass dichroic mirror. The infrared portion of the spectrum was further split by a nonpolarizing 50/50 beamsplitter. Each of the three paths was further spectrally filtered prior to detection by single photon detectors to guarantee no spectral overlap. The spectral ranges of the filters used are marked on top of a typical single QD emission spectrum in Figure 3a as green and red regions.

The emission spectrum of a single QD, given in Figure 3a, clearly shows two spectrally distinct emission bands with

dx.doi.org/10.1021/nl300638t | *Nano Lett.* 2012, 12, 2948–2952

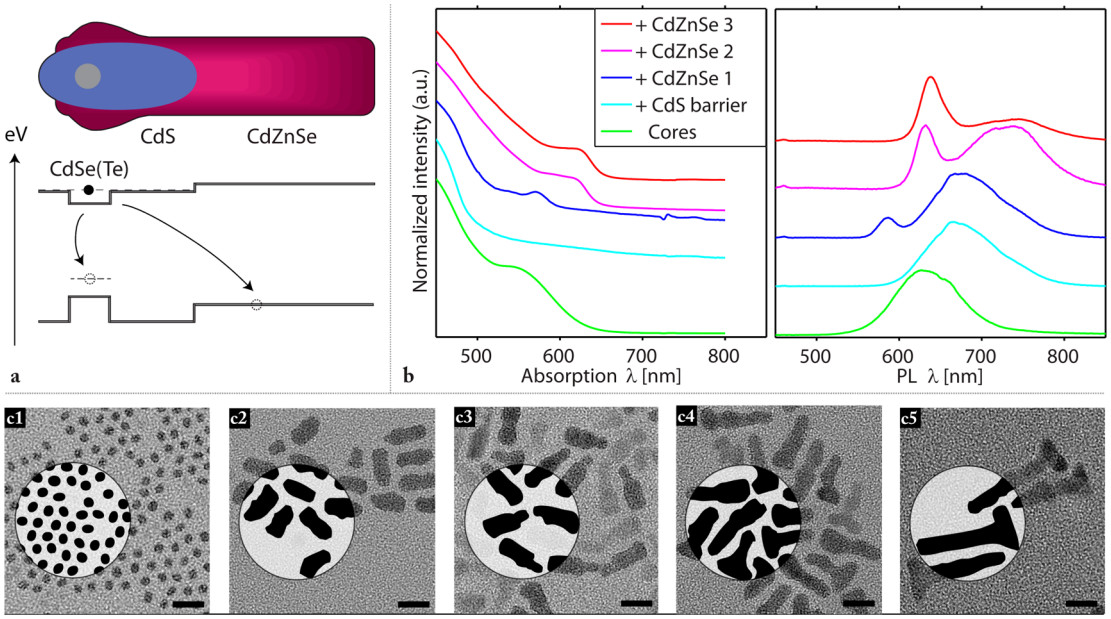

Figure 2. Synthesis of dual-emitting quantum dots. (a) A schematic illustration of the QD structure. The CdSe(Te) core is portrayed in gray, the CdS barrier in blue and CdZnSe is red. The gradient in the shade of red captures the various stages of CdZnSe growth, where the lighter shade signifies earlier stages. Shown in the bottom is a schematic energy diagram of the QD aligned with the structure on top. (b) Absorption and emission spectra from five stages of the synthesis (cores only, growth of CdS barrier and three stages of CdZnSe growth). Consecutive spectra are vertically shifted for clarity. (c) TEM images of QDs from the five stages introduced in b. Scale bars are 10 nm. A graphical mask of the particles in each image is overlaid with a small region of the original TEM image to guide the eye. CdZnSe can be seen to grow initially as a thin extension protruding from the rodlike particles of stage 2. Further growth leads mostly to the lengthening and thickening of this protrusion. Additional lobes form on the opposite end of the rods at later stages of the synthesis.

maxima at 597 nm (Vis) and 706 nm (NIR). Emission transients for both emission colors, obtained by histogramming time-correlated single photon counting data, are given in Figure 3b. While the NIR emission shows single exponential decay with a lifetime of 140 ns, the Vis emission is nonexponential and has a shorter lifetime. A common feature of single QDs is their tendency to exhibit PL intermittency (see also in the Supporting Information).[22] In this context, the lifetime curves shown in Figure 2b are of the "On" times. "Off" times are filtered out by thresholding with 100 ms time bins.

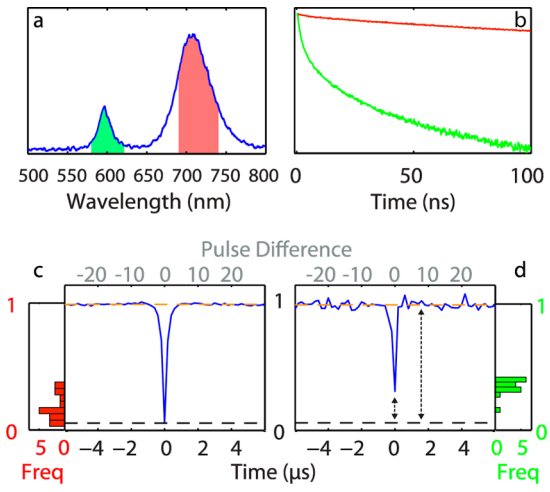

Figure 3. Optical characterization of a single dual color emitting QD. (a) QD emission spectrum, exhibiting two well separated peaks. The spectral filters used for correlation experiments are overlaid on the spectrum. (b) Emission lifetimes of the two colors on a semi-logarithmic scale. NIR emission is nearly single exponential with $\tau \sim$ 140 ns. The Vis emission is multiexponential exhibiting a long emission tail. (c) NIR−NIR emission autocorrelation trace, exhibiting a deep antibunching dip. The dashed black line depicts the minimal simultaneous-pair count for this setup considering detector dark counts. (d) The Vis−NIR emission cross-correlation trace similar to that presented for NIR−NIR. Histograms of antibunching dip depths for 17 different QDs are plotted adjacent to traces c and d.

To unequivocally prove that the observed object is indeed a single QD, we first consider the emission statistics of the NIR emission peak. Because of the relatively small size of the CdSe core and due to Te doping, the NIR peak should exhibit fast Auger decay and correspondingly nearly full antibunching. Indeed, the second order autocorrelation function of NIR emission $[g^{(2)}(\tau)]$ (analyzed with a bin size equal to the interval between consecutive pulses), shown in Figure 3c, exhibits a deep dip at $\tau = 0$. The dip almost reaches the minimal level of bunched photon pairs given the detector dark count rate (dashed black line), which indicates that most of the NIR photons emanate from a single quantum emitter.

To demonstrate that the Vis emission also originates from the same object, we turn to look at the second order cross-correlation curve of the Vis and NIR photons, shown in Figure 3d. Just as for the NIR emission, there is a minimum at $\tau = 0$. This curve demonstrates significant anticorrelation between the two emission colors; simultaneous emission of a NIR photon and a Vis photon is deeply suppressed. Histograms of the dip depth for 17 different QDs are also plotted alongside Figures 3c,d. Most importantly, all QDs exhibit a dip depth well below 0.5, clearly indicating that all observed QDs are single two-color emitters.

The shape of the two-color cross-correlation curve was typically asymmetric as shown in Figure 3d. Pairs with a Vis photon preceding a NIR photon exhibited a slower increase,

dx.doi.org/10.1021/nl300638t | Nano Lett. 2012, 12, 2948−2952

which corresponds to the longer relaxation time observed for the NIR emission. The characteristic delay at which antibunching disappears for positive and negative delays agrees with the decay times of the NIR and Vis channel, respectively. This implies that the observed anticorrelation is indeed due to exciton−exciton interactions rather than to photochromic dynamics of the emitter.

In the above analysis, the Vis photons detected are time-selected (for $\tau > 20$ ns) to exclude the relatively rapid initial decay transient. This is required since at short times after the pulse the Vis emission is dominated by photons from multiexcitonic cascades, which naturally reduce antibunching as will be explained below. We therefore now turn to characterize the transient dynamics governing two-color antibunching.

Multiexciton relaxation taking place in the QD is a competition between the radiative decay and the nonradiative Auger recombination. Since Auger recombination is faster by an order of magnitude it is a far more probable relaxation route. However, since relaxation is a stochastic process, a small fraction of multiexcitons nonetheless undergo radiative recombination and therefore in these cases more than one photon per pulse is emitted. Naturally, this results in reduced antibunching since pairs of photons are emitted at short time lags.

To further explore the effect of multiexciton emission on the correlation of the Vis and NIR emissions, photons can be filtered by delay from the excitation pulse. Since photons originating in multiexciton recombination tend to arrive at shorter delays, discriminating the early arriving photons increases the antibunching feature in the cross-correlation curves.

To quantify this, we characterize the intrinsic level of two-color antibunching, taking into account detector dark counts that lead to observation of false coincidence events. To this end, we define the degree of bunching Q

$$Q(\%) = \left(\frac{G^{(2)}(\tau = 0) - N}{G^{(2)}(\tau \neq 0) - N}\right)100$$

where $G^{(2)}(\tau = 0)$ is the observed number of photon pairs with zero delay and N is the estimated number of coincidence events due to detector dark counts. $G^{(2)}(\tau \neq 0)$ is the average number of coincidence events with a delay in the range −30 to +30 pulses, excluding the central region from −3 to +3 pulses. The numerator and denominator of this formula are graphically depicted in Figure 3d by the short and long arrows, respectively. Under this definition full antibunching is quantified by $Q = 0$ while completely uncorrelated signals yield $Q = 100$ and photon bunching will result in $Q > 100$.

The effect of filtering photons with short delay times on the degree of bunching is presented in Figure 4b. One can see that, indeed, exclusion of early arriving photons significantly decreases the degree of two-color bunching (Q). An indication that this effect is primarily related to multiexcitons is given by its dependence on the excitation intensity, as presented in Figure 4e. Increasing the excitation intensity increases the probability of creating multiexcitons and as a result, antibunching becomes less pronounced at the higher excitation power when no filtering is done (the value of Q for high power curve reaches a higher value than the low power curve in Figure 4e). However, once photons originating from multiexciton

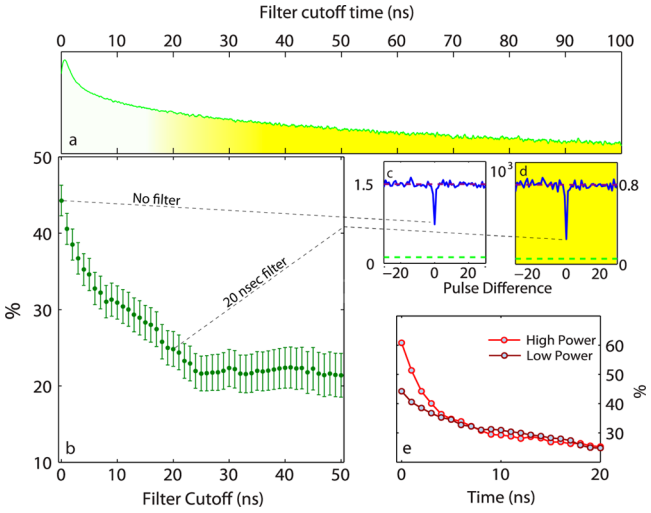

Figure 4. Dependence of antibunching level on the temporal filter threshold. (a) Typical lifetime curve of the Vis photons aligned with the plot described in b. (b) Dependence of the degree of bunching (Q) on the delay-time threshold used for the filtering of Vis photons. There is a clear improvement of antibunching as the threshold increases from 0 to 20 ns. In our analysis, we used photons arriving from 20 ns onward as indicated by the yellow shading on the lifetime curve (note that the full lifetime curve, extending to 200 ns, is not shown in the figure). (c,d) Cross correlation curves, without (c) and with (d) the 20 ns threshold filter. The dashed lines connect each curve to its respective antibunching level on the plot in b. (e) Curves of degree of bunching vs delay-time thresholds for high (15 μJ/cm^2·pulse) and low (2.4 μJ/cm^2·pulse) excitation powers. The high power curve diverges from the low power curve at very short threshold onsets (~3 ns) consistent with the picture of antibunching getting worse as more multiexcitons are formed.

cascades are filtered out the value of Q converges to the level of antibunching observed for lower excitation intensities.

Finally, we show that two color antibunching is a general feature of this system demonstrated by a vast majority of the surveyed NCs. Histograms of the degree of bunching (Q) for NIR autocorrelation and two-color cross-correlation using data from 17 QDs are presented in Figure 5. QDs that were

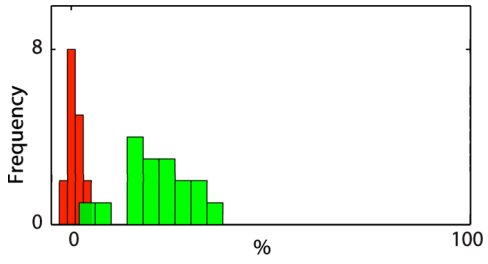

Figure 5. Histograms of the degree of bunching (Q) from an ensemble of 17 dual-color emitting QDs after processing. Histograms take into account detector dark counts for both the NIR−NIR autocorrelation traces (red), and for the Vis−NIR cross-correlation traces (green).

accounted for in this histogram were chosen solely on the basis of high signal-to-noise ratio. The red histogram reflects the fact that every QD inspected exhibited nearly full antibunching of the NIR photons with about 4% on average. The two-color antibunching seen on the NIR/Vis cross correlation curve, although not complete, is very significant, reaching on average less than 20% and is clearly a typical characteristic of this dual

dx.doi.org/10.1021/nl300638t | Nano Lett. 2012, 12, 2948−2952

emitting composite nanostructure. A probable explanation for the incomplete antibunching may lie in the presence of smaller CdZnSe islands disconnected from the main CdZnSe rod, as observed most clearly in Figure 2c5, complicating the simplified scheme portrayed in Figure 1c.

We have shown that structures with a relatively complicated design can be readily realized by colloidal synthesis and demonstrated how engineering of a composite QD fluorophore can lead to desired optical properties, in particular two-color antibunching. This is an important step toward achieving novel, significantly more complex forms of nonclassical light. For example, increasing the number of coupled emitters and refining the details of the coupling mechanisms, one can readily envision generation of higher-order mutually exclusive photon emission at multiple colors. Moreover, an extension of the modular design introduced here, taking advantage of the pairwise Auger interaction, should allow for emission of photon pairs of one type anticorrelated with pairs of a different kind.

Interaction engineered quantum emitters, such as the ones presented here, can enable novel applications, such as the darkening of the Vis channel by optically pumping in the NIR channel.[14] Such room-temperature control of the emission flux could be used in the framework of stimulated emission depletion (STED) superresolution microscopy technique,[23] where a doughnut-shaped NIR beam will inhibit Vis emission at the peripheral regions of the excitation point spread function, practically localizing the excited area beyond the diffraction limit.

Another attractive application of engineered nanocrystal emitters is photon upconversion, a process that attracted attention due to its possible use in solar cells.[24] Similarly to organic systems exhibiting photon upconversion via mechanisms such as triplet−triplet annihilation,[25] exploitation of Auger recombination to generate a single high energy exciton out of several low energy exictons in multicolor emitting QDs is a viable pathway for efficient photon upconversion in a solid state system. In conclusion, we believe this study opens a broad range of applications in photonics for "designer" colloidal QD heterostructures.

■ ASSOCIATED CONTENT

Supporting Information

Detailed description of the synthesis process; correlation measurement setup description; photoluminescence excitation (PLE) measurements; fluorescence intermittency results; detailed description of data analysis and error estimation; and detailed description of quantum yield characterization. This material is available free of charge via the Internet at http://pubs.acs.org.

■ AUTHOR INFORMATION

Corresponding Author

*E-mail: Zvickad@gmail.com.

Notes

The authors declare no competing financial interest.

■ ACKNOWLEDGMENTS

Z.D. would like to extend his gratitude to J. Van Embden for his patience and his priceless advice on synthetic methods. Financial support by the European Research Council starting investigator Grant SINSLIM 258221, the Israeli ministry of science Tashtiyyot program, the Crown center of photonics and the Irving and Cherna Moskowitz Center for Nano and Bio-Nano Imaging is gratefully acknowledged. O.S. is supported by the Adams Fellowship Program of the Israel Academy of Science and Humanities. D.O. is the incumbent of the Recanati career development chair in energy research.

■ REFERENCES

(1) Hanbury Brown, R.; Twiss, R. Q. *Proc. R. Soc. London* **1957**, *242*, 1230.
(2) Lounis, B.; Orrit, M. *Rep. Prog. Phys.* **2005**, *68*, 1129−1179.
(3) Morgan, B. L.; Mandel, L. *Phys. Rev. Lett.* **1966**, *16*, 1012−1015.
(4) Kimble, H. J.; Dagenais, M.; Mandel, L. *Phys. Rev. Lett.* **1977**, *39*, 691−695.
(5) Mandel, L. *Opt. Lett.* **1979**, *4*, 7.
(6) Th. Basche, W. E.; Moerner, M.; Orrit, H. T. *Phys. Rev. Lett.* **1992**, *69*, 1516−1519.
(7) Kurtsiefer, C.; Mayer, S.; Zarda, P.; Weinfurter, H. *Phys. Rev. Lett.* **2000**, *85*, 290−293.
(8) Michler, P.; Imamoglu, A.; Mason, M. D.; Carson, P. J.; Strouse, G. F.; Buratto, S. K. *Nature* **2000**, *406*, 968−970.
(9) Lounis, B.; Bechtel, H. A.; Gerion, D.; Alivisatos, P.; Moerner, W. E. *Chem. Phys. Lett.* **2000**, *329*, 399−404.
(10) Santori, C.; Pelton, M.; Solomon, G.; Dale, Y.; Yamamoto, Y. *Phys. Rev. Lett.* **2001**, *86*, 1502−1505.
(11) Akopian, N.; et al. *Phys. Rev. Lett.* **2006**, *96*, 130501.
(12) Shields, A. J. *Nat. Photonics* **2007**, *1*, 215−223.
(13) Berglund, A. J.; Doherty, A. C.; Mabuchi, H. *Phys. Rev. Lett.* **2002**, *89*, 068101.
(14) Fuckel, B.; Hinze, G.; Nolde, F.; Mullen, K.; Basche, T *Phys. Rev. Lett.* **2009**, *103*, 103003.
(15) Hofkens, J.; et al. *Proc. Natl. Acad. Sci. U.S.A.* **2003**, *100*, 13146−13151.
(16) Hubner, C. G.; Zumofen, G.; Renn, A.; Herrman, A.; Mullen, K.; Basche, T. *Phys. Rev. Lett.* **2003**, *91*, 093903.
(17) Battaglia, D.; Blackman, B.; Peng, X. *J. Am. Chem. Soc.* **2005**, *127*, 10889−10897.
(18) Dias, E. A.; Petrik, A.; English, D. S.; Kambhampati, P. *J. Phys. Chem. C* **2008**, *112*, 14429.
(19) Klimov, V. I.; Mikhailovsky, A. A.; McBranch, D. W.; Leatherdale, C. A.; Bawendi, M. G. *Science* **2000**, *287*, 1011−1013.
(20) Avidan, A.; Oron, D. *Nano Lett.* **2007**, *8*, 2384−2387.
(21) Sitt, A.; Della Sala, F.; Menagen, G.; Banin, U. *Nano Lett.* **2009**, *9*, 3470−3476.
(22) Nirmal, M.; et al. *Nature* **1996**, *383*, 802−804.
(23) Hell, S. W. *Science* **2007**, *316*, 1153−1158.
(24) Ekins-Daukes, N. J.; Schmidt, T. W. *Appl. Phys. Lett.* **2008**, *93*, 063507.
(25) Islangulov, R. R.; Kozlov, D. V.; Castellano, F. N. *Chem. Commun.* **2005**, *30*, 3776−3778.